



Communication

Intrinsic half metallicity in lithium terminated zigzag graphene nanoribbons

Neha Tyagi^{a,*}, Neeraj K. Jaiswal^b, Varun Sharma^c, Kamal K. Jha^d, Pankaj Srivastava^c^a Department of Applied Physics, Delhi Technological University, Delhi 110042, India^b Discipline of Physics, Indian Institute of Information Technology, Design & Manufacturing, Jabalpur, Dumna Airport Road, Jabalpur 482005, India^c Nanomaterials Research Group, ABV-Indian Institute of Information Technology & Management, Gwalior 474015, India^d Indian Institute of Information Technology, Vadodara 382028, India

ARTICLE INFO

Keywords:

A. Graphene nanoribbon
 A. Lithium
 D. Binding energy
 D. Half-metal
 D. Spintronic

ABSTRACT

Half-metallic materials are the prime requisite for future spintronic devices. In present work, the possibility of half-metallic characteristic has been investigated in Li terminated zigzag graphene nanoribbons (ZGNR) using density functional theory. Two different configurations: (i) both edges Li termination (Li-both edges) and (ii) one edge Li termination (Li-one edge), have been examined in the present study. The calculated binding energy (ranging from -3.19 eV to -4.96 eV) confirms that both the considered configurations are energetically viable to obtain. All the considered structures settled in antiferromagnetic ground state which is more stable than that of spin compensated state. Further, it is revealed that upto 100% spin polarization can be achieved (without application of any external electric field) in ZGNR with Li-one edge. Moreover, the observed half-metallicity is found to be independent of the ribbon width and therefore pledges for applications in novel spin filtering devices.

1. Introduction

The search of novel materials for improved generation of future electronic devices is an area of active research. Nano-materials like graphene, a perfect 2-D sheet of carbon atoms [1,2], exhibit great potential for beyond Si electronic devices [3–6]. Moreover, future devices are supposed to be faster, smaller as well as eco-friendly in nature [7–9]. To meet these requirements, low power consumption is one of the important criteria decides the adaptability of any device. Progressing in this direction, researchers are also investigating the new class of devices known as spintronic devices [10–12]. The spintronic devices will be governed by the electron spin rather than its charge as in conventional electronic devices. The prime requirement of these proposed spintronic devices are the materials that can differentiate the spin up electrons with those of spin down. Such materials, formally known as the half-metals, are rare to be found. However, researchers have shown that zigzag graphene nanoribbons (ZGNR) exhibit half-metallic properties in the presence of external electric field [13]. In other studies, it is revealed that the spin filtering properties (half metallicity) can be induced in ZGNR via doping of selective impurities at predefined sites [14–16]. Despite of these efforts, still the obtained spin polarization is not very promising. Although few reports are available to claim up to 100% spin polarization in GNR but it requires controlling the doping sites with atomic precision [16–19]. To obtain

such structures, first we need to create a vacancy in the GNR network and then fill these vacant sites with guest atoms which make it difficult to experimentally realize these half-metallic GNR. Previous findings revealed that edge termination of GNR by metal atoms is energetically more favourable than the substitutional doping of the ribbons with same metal [18]. In the present work, we have investigated the possibility of half-metallicity in Li-terminated ZGNR and found promising results. The selection of Li is based on the fact that it can replace terminating H atoms at the edges of ZGNR due to its higher position (than that of H) in electro chemical series. Further, the edge termination is comparatively easier to control than that of substitutional doping by metal atoms. This indicates towards the practical viability of the proposed configurations to realize half-metallicity in GNR.

2. Computational details

The proposed structures of Li-terminated ZGNR have been investigated using density functional theory (DFT) based first-principle calculations [20,21]. The considered geometries have been modelled by using supercell approach. Owing to the quasi 1-D geometry of ribbons, the periodicity of the structures was maintained along Z-axis whereas the remaining two directions were kept confined. The k-point sampling of $1 \times 1 \times 50$ points in Monkhorst Pack scheme [22] along with

* Corresponding author.

E-mail address: nehatyagi@dtu.ac.in (N. Tyagi).

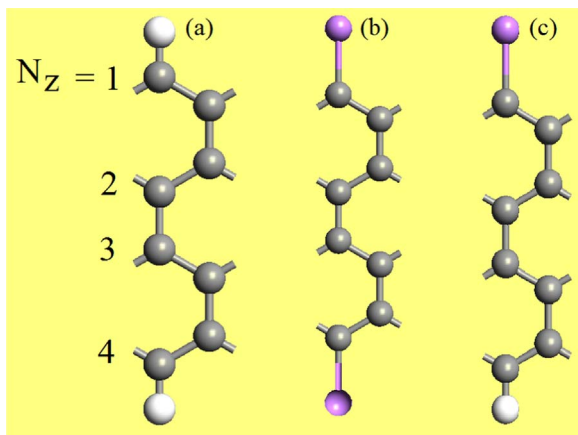


Fig. 1. The convention of defining the width of ZGNR and the considered structures of (a) Pristine ZGNR (b) Both edges Li terminated ZGNR (c) One edge Li terminated ZGNR. The grey, white and purple spheres represent C, H and Li atoms respectively.

Table 1

The calculated binding energy (BE), magnetic stabilization ($E_{\text{AFM}} - E_{\text{NM}}$), spin induced energy band gap (E_{sg}) as a function of ribbon widths.

Width (N_z)	Configuration	BE (eV)	$E_{\text{AFM}} - E_{\text{NM}}$ (meV)	E_{sg} (eV)
4	Pristine	−6.58	60.5	0.64
	Li-both edges	−3.19	115.2	0
	Li-one edge	−4.93	83.6	0.72
6	Pristine	−6.59	70.1	0.57
	Li-both edges	−3.22	118.2	0
	Li-one edge	−4.94	95.2	0.68
8	Pristine	−6.59	70.2	0.51
	Li-both edges	−3.23	120.1	0
	Li-one edge	−4.96	98.7	0.65

cut off energy of 70 Rydberg was used for the geometry optimization. Further, a vacuum region of 10 Å was also introduced in the supercell along X and Y directions to prevent interactions of structures with their replica. In order to account the exchange and correlation energy, we used generalised gradient approximation (GGA) with Perdew-Burke-Ernzerhof (PBE) parameterization [23]. For all the present calculations, double zeta plus polarized basis set was employed. The optimization was done self-consistently and cycle of optimization was continued taking the maximum force component of 0.04 eV/Å as the optimization criteria. Once, geometry has been optimized, the band structures and density of states (DOS) were computed with higher number of k -points.

Moreover, to take width effects in to account, we considered ZGNR having widths from $N_z = 4$ to $N_z = 8$. The nanoribbons width was defined equal to number of C-C pairs across the width. Present investigated structures are (i) both edges Li termination (Li-both edges) and (ii) one edge Li termination (Li-one edge). The width convention along with the schematics of considered structures is depicted in Fig. 1. For the calculation of transport properties, we used optimized geometries in two-probe configuration. The central channel region in two-probe geometry, between left and right electrodes, is seamlessly coupled with semi-infinite electrodes to avoid interface scattering at both the ends. The transport calculations were performed using the same parameters and models as explained in Ref. [24].

3. Results and discussion

In the present study, structural and spintronic properties of ZGNR interacting with Li atoms as terminating elements, have been investigated. It is noticed that after optimization, ribbons adhere to their perfectly planar structure for Li-both edges as well as for Li-one edge. The terminating Li atoms form stable chemical bonds with the edge C atoms. The optimized Li-C bond length was found to be 1.97 Å which is consistent with the previous theoretical predictions [25]. It is revealed that Li-terminated ZGNR exhibit magnetic ground state. All the considered structures favour antiferromagnetic (AFM) coupling between edges which is about ~115–120 meV more stable than that of nonmagnetic (NM) state in Li-both edges. For Li-one edge this difference ranges ~83–98 meV. Similar AFM coupling has been noticed previously for pristine ZGNR [26]. The observed magnetic coupling is greater than that of the pristine ribbons [Table 1]. In order to examine the origin of observed magnetic ground state, we analysed spin compensated DOS for Li-both edges and Li-one edge ribbons as shown in Fig. 2(a) and 2(b) respectively. As the findings are similar, to be concise, the DOS have been depicted only for $N_z = 4$. In both the cases, a sharp peak is noticed at the Fermi level which indicates that observed magnetic ground state arises due to magnetic stabilization. Moreover, the characteristic 1-D behavior is also evident from the DOS profiles [shown by arrows in Fig. 2]. The observed magnetic stabilization ($E_{\text{AFM}} - E_{\text{NM}}$) of Li terminated ZGNR is presented in Table 1. Owing to this magnetic stabilization, splitting of electronic states takes place near the Fermi level which in turn gives rise to AFM ground state. The similar magnetic stabilization was previously observed for pristine ZGNR due to availability of sharp edge states at the Fermi level [26].

After determining most stable ground state, we next compared the structural stability of ribbons on the basis of binding energy (BE) calculations. The analysis of BE indicates that Li-one edge is energetically more favourable than Li-both edges [Table 1]. The similar

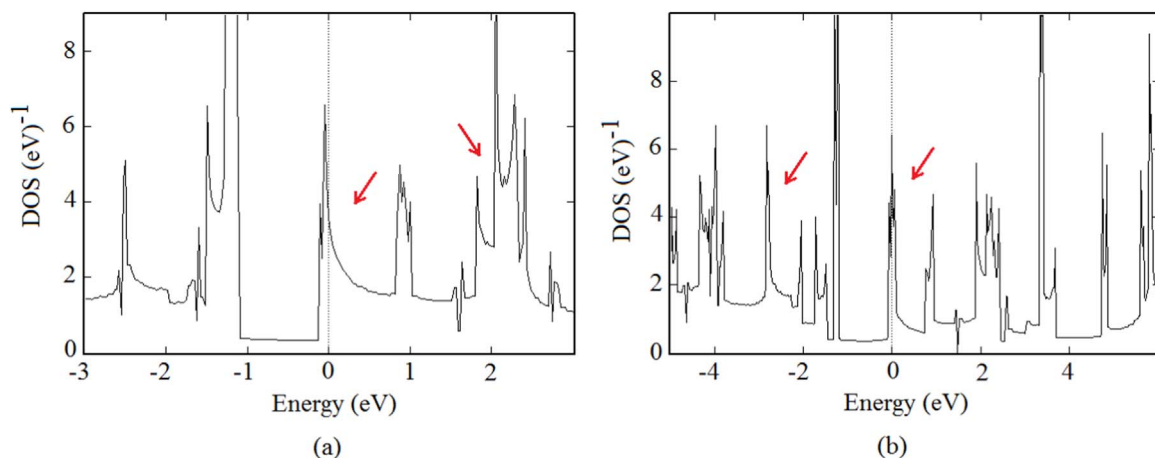


Fig. 2. Spin compensated density of states (DOS) profiles for (a) Both edges Li terminated ZGNR and (b) One edge Li terminated ZGNR. The dotted line at 0 eV represents the Fermi level.

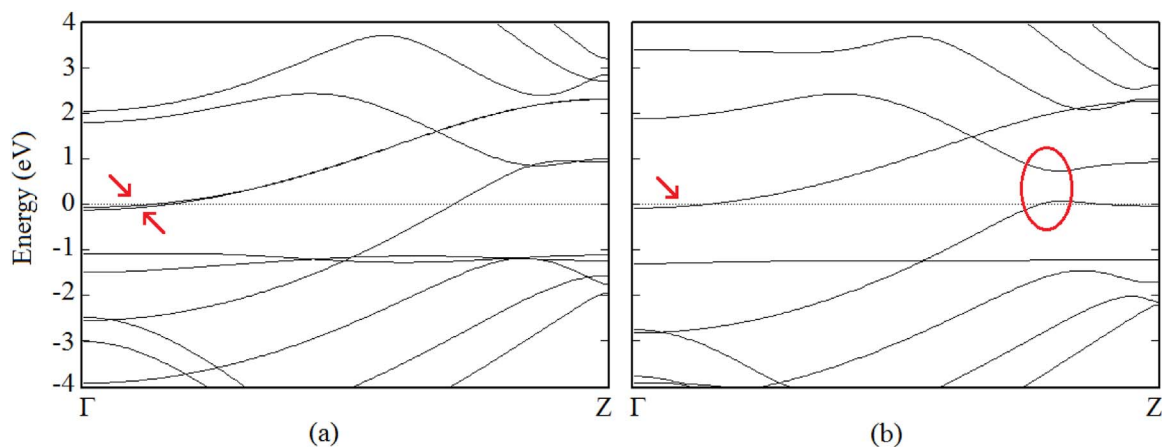


Fig. 3. The spin compensated band structures ($N_z=4$) for (a) Both edges Li terminated ZGNR and (b) One edge Li terminated ZGNR configurations. The dotted line at 0 eV represents the Fermi level.

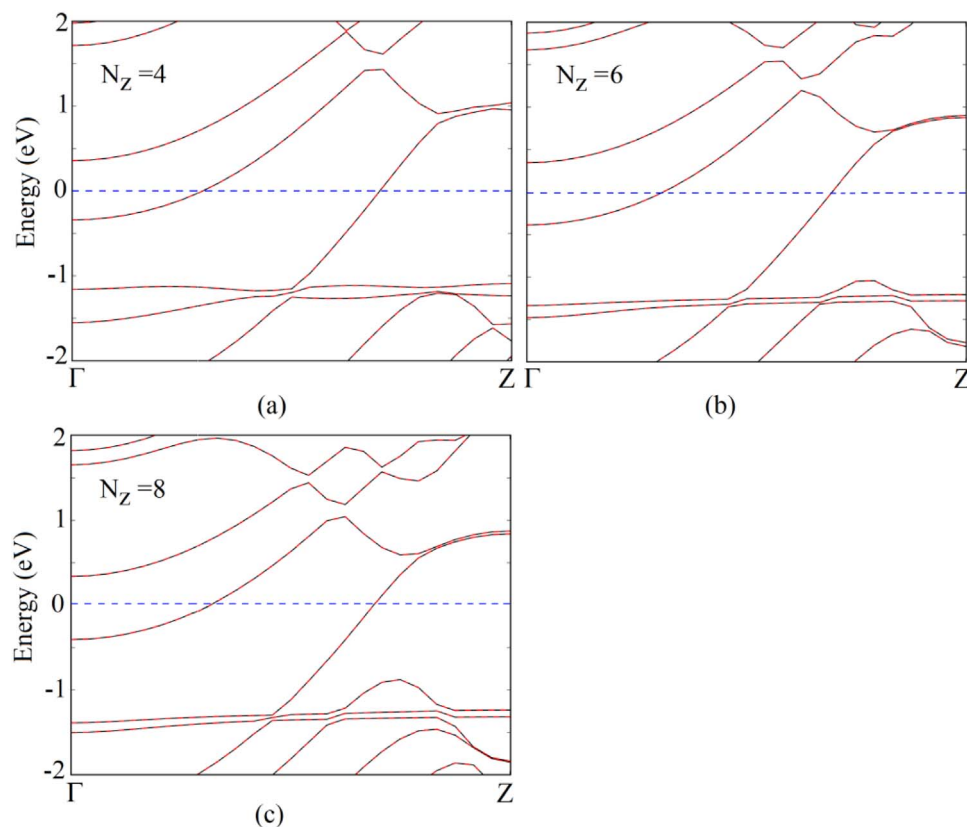


Fig. 4. The spin polarized band structures of both edges Li terminated ZGNR for (a) $N_z=4$ (b) $N_z=6$ and (c) $N_z=8$. The dashed line at 0 eV represents the Fermi level.

findings were obtained for ZGNR interaction with transition metals [24]. It is also noticed that widths do not play a significant role for structural stabilities of the configurations. This is due to the fact that chemical bonding between terminating Li and edge C atom is mediated via charge transfer at local level. For Li-both edges, 0.01e charge transfer takes place between Li and the nearest C atom. On the other hand, for Li-one edge, the edge C atom (bonded with Li) receives 0.023e charge from Li at one edge and donates 0.08e to the terminating H atom at opposite edge. Owing to this unequal charge transfer at opposite edges, the degeneracy of edge states is no more preserved in Li-one edge ZGNR as highlighted by the circle [Fig. 3(b)]. However, the equal charge transfer at opposite edges preserves the electronic states degeneracy in both edges Li terminated ZGNR as shown in Fig. 3(a) for representative width $N_z=4$. Further, each terminating Li atom contributes an additional electronic band near the Fermi level. For

Li-both edges two such bands are observed whereas for Li-one edge only one additional band appears across the Fermi level as highlighted by arrows [Fig. 3(a)-(b)].

To investigate the spin dependent electronic properties of ribbon, we calculated spin polarized band structures and corresponding DOS. For Li-both edges, we observed that band structures exhibit degenerate energy states [Fig. 4(a)-(c)]. Further, a number of conducting channels are noticed across the Fermi level which indicates their metallic behavior irrespective of ribbon width. The corresponding DOS and partial DOS (PDOS) have been presented in Fig. 5 for $N_z=4$. As expected from the preserved spin degeneracy of the energy states in band structures of Li-both edges, we observed equal and symmetric DOS for spin up and spin down electrons. Further, availability of DOS across the Fermi level further confirms its metallic character. Thus, for both edges Li-terminated structures, both types of spin play equal role

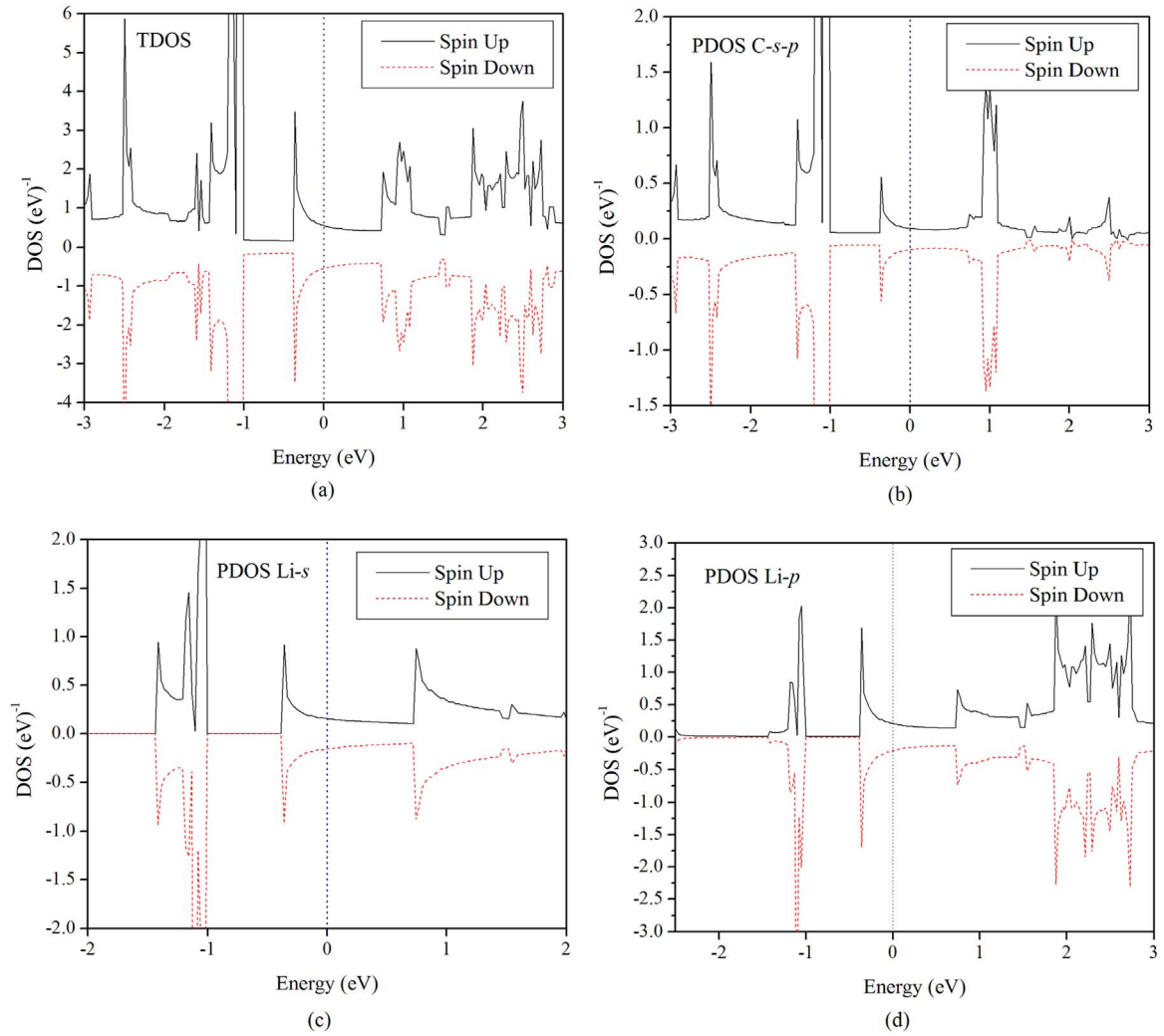


Fig. 5. The spin polarized DOS ($N_z = 4$) for both edges Li terminated ZGNR (a) Total DOS (TDOS) and the partial DOS (PDOS) for (b) s and p orbital of edge C atoms (c) s orbital of Li (d) p orbital of Li. The vertical dashed line at 0 eV represents the Fermi level.

towards the current conduction.

On the other hand, the spin polarized band structures of Li-one edge [depicted in Fig. 6(a)–(c)], revealed broken degeneracy between opposite spin electrons. It is observed that Li-one edge turns the ribbon half-metallic (i.e. metallic for spin up electrons whereas semiconducting for spin down electrons). The broken degeneracy of electronic states is due to asymmetry of ribbons and hence, unequal charge transfer taking place at opposite edges. The Li terminating edge receives charge from terminating (Li) atom whereas opposite edge donates charge to the terminating H. Thus, an electrostatic potential difference is developed between opposite edges of ribbon. The π orbital of edge C atoms shift under the influence of this potential [27] which pushes the spin up and spin down electronic states in opposite directions and ultimately results into half-metallic character. Similar effect was also used to induce half metallicity in ZGNR by Wu et al. [28]. However, they could make half-metallic ZGNR only for wider ribbons having width $N_z > 16$. On contrary, the half metallicity proposed in the present work persists for widths as narrow as $N_z = 4$. The considered ribbons ($N_z = 4, 6, 8$) are found to be metallic (semiconducting) for spin up (spin down) electrons. However, it is observed that for narrow ribbons, the highest valence band (HVB) for spin down electrons lie in the vicinity of Fermi level compared to that of wider ribbons. This is due to the fact that edges of ZGNR are under the influence of two competing effects (i) AFM coupling between opposite edges and (ii) the developed potential difference (arises due

to charge donated at one edge and received at opposite edge). For narrow ribbons the AFM coupling is prevailing whereas for wider ribbons the developed potential difference becomes more effective. Therefore, HVB for spin down electron is shifted downward upto a greater extent in wider ZGNR. Further, the spin induced band gap (E_{sg}) is indirect in nature for all the widths and corresponding magnitude is presented in Table 1.

In order to understand the origin and behavior of observed half metallicity in one-edge Li-terminated ribbons, the DOS and PDOS have also been analysed as depicted in Fig. 7. For Li-one edge structures, the DOS exhibits finite availability (absence) of states at the Fermi level for spin up (spin down) electrons. Since the findings are not affected by the ribbon width, to be concise, here we have shown DOS and PDOS plots only for $N_z = 4$. The half metallic gap of ~ 0.72 eV across the Fermi level for spin down states corresponds to observed electronic band structure [Fig. 6(a)]. Further, it can be noticed that electronic states are asymmetric for opposite spins which is due to broken spin degeneracy of the electronic states. Analysis of PDOS reveals that highest valence band peak for spin down states is mainly due to edge C atoms [Fig. 7(b)]. On the other hand, conduction band peaks are collective contribution of p-orbital of C and the terminating Li. Since this configuration is metallic for one type of spin and semiconducting for opposite spin, the structure acts as half-metal and is ideal for novel spin filtering devices. Here, 100% spin polarization is observed which indicates great potential of these structures for spintronic devices.

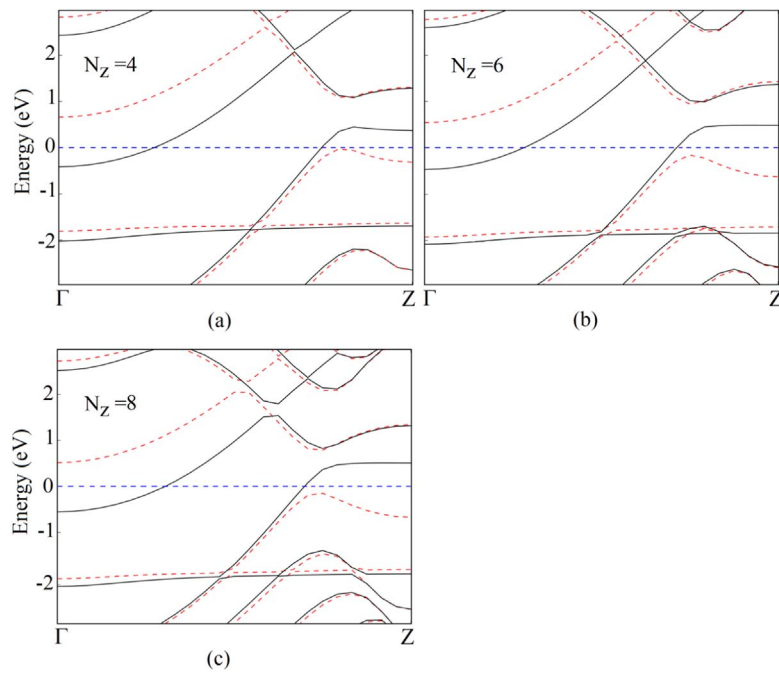


Fig. 6. The spin polarized band structures of one edge Li terminated ZGNR for (a) $N_z = 4$ (b) $N_z = 6$ and (c) $N_z = 8$. Solid (black) and dashed (red) lines represent the electronic states for spin up and spin down electrons respectively. The metallic behavior for spin up and semiconducting for the spin down electrons is evident for all considered nanoribbons width i.e. $N_z = 4$ –8. The dashed line at 0 eV represents the Fermi level (For interpretation of the references to color in this figure legend, the reader is referred to the web version of this article.).

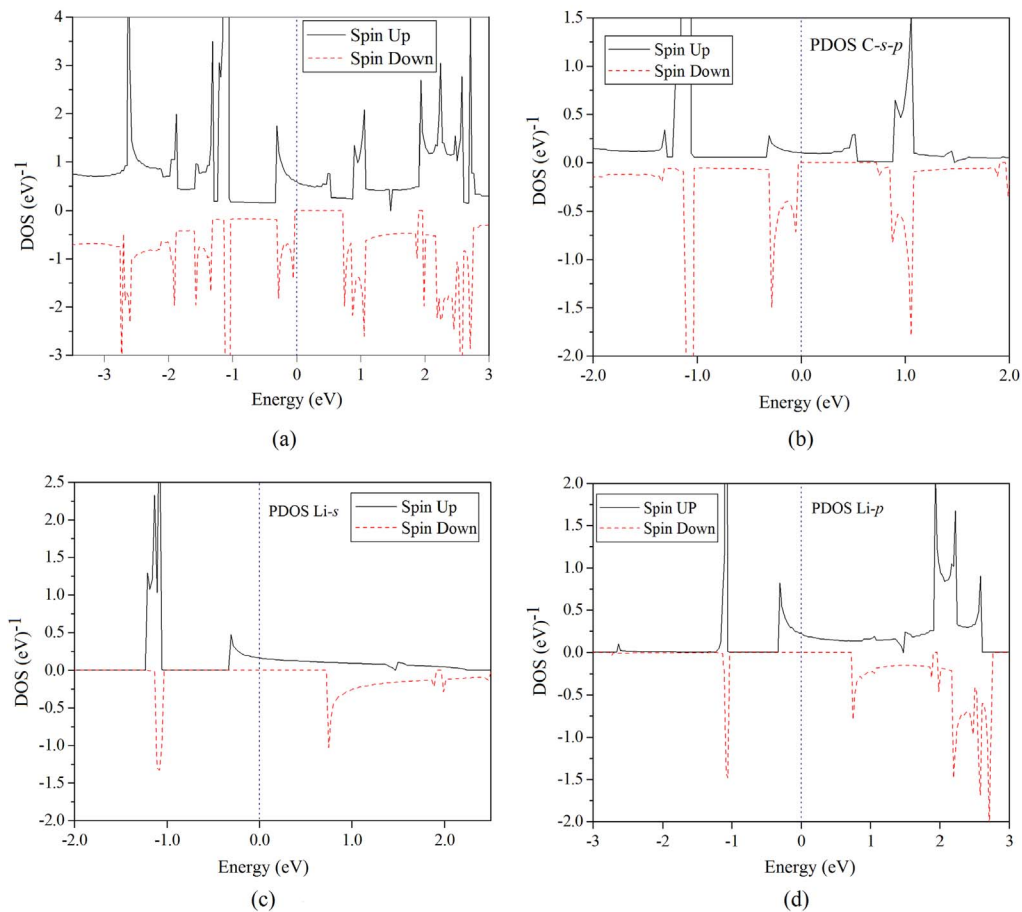


Fig. 7. The spin polarized DOS ($N_z = 4$) for one edge Li terminated ZGNR (a) TDOS and the PDOS for (b) s and p orbital of edge C atoms (c) s orbital of Li (d) p orbital of Li. The vertical dashed line at 0 eV represents the Fermi level.

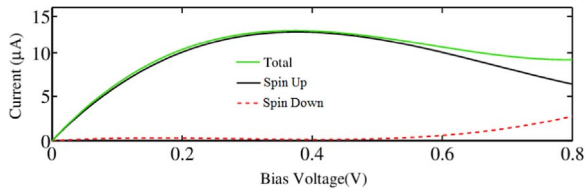


Fig. 8. The calculated I - V characteristic of half-metallic ZGNR ($N_z = 4$).

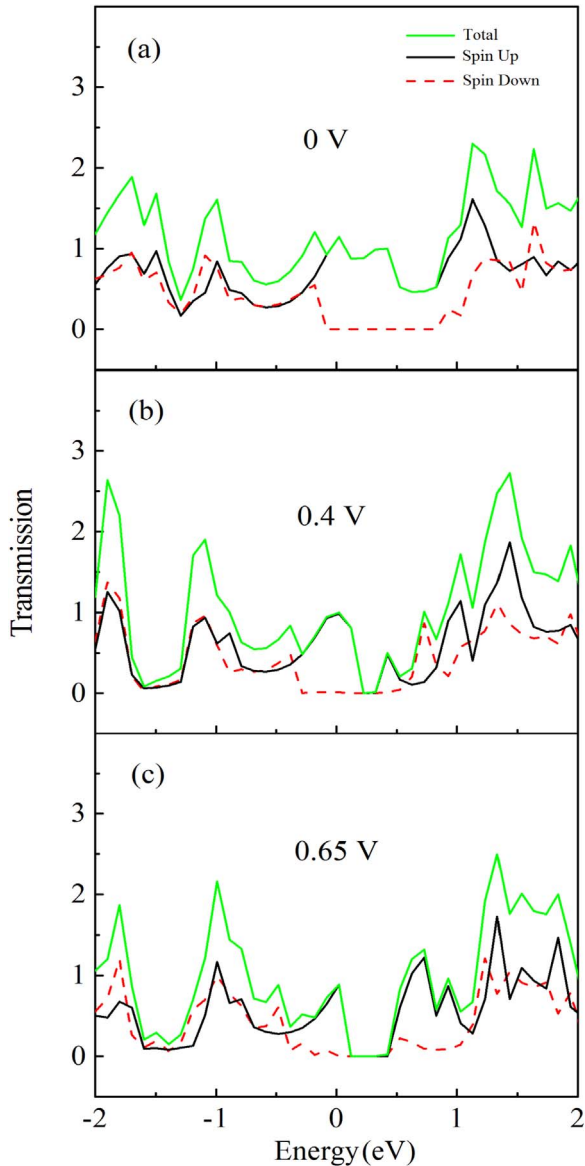


Fig. 9. The transmission spectra of half-metallic ZGNR ($N_z = 4$) for the bias voltages as mentioned therein.

Further, termination is comparatively easier to control as compared to selective doping (with foreign atoms), making it more simple and viable way to achieve high spin polarization. Another advantage of the present finding is that no external electric field is required to observe half metallic character in contrast to that of pristine ZGNR [13].

To demonstrate the spin filtering capability of Li-one edge ribbons, we have also calculated current-voltage (I - V) characteristics using two-probe models as adopted in previously [29]. The obtained I - V behavior has been plotted in Fig. 8 (for $N_z = 4$). As expected, with increasing the applied bias voltage, current starts to increase for spin up electrons which is in consistent with its metallic behavior of spin up electrons.

On the other hand, current remains negligible for spin down electrons until the applied bias exceeds spin induced band gap as shown by red dashed lines in Fig. 8. Since the spin dependent band gap (~ 0.72 eV) is sufficiently larger than that of room temperature excitation energy (~ 0.025 eV), it is evident that Li-one edge ZGNR can act as a perfect spin filter. Such a spin filtering capability in the absence of any external electric field is of great importance for designing future memories and spin filtering devices.

For a further understanding of the observed I - V characteristics, we computed the transmission spectra (TS) for Li-one edge ($N_z = 4$) for different bias voltages as depicted in Fig. 9. The perusal of TS indicates that for spin down states, value of transmission coefficient is zero in the vicinity of Fermi level which is in consistent with the observed semiconducting behavior for spin down electrons. The current conduction is taking place only via spin up electrons. Therefore, TS further verifies the spin filtering capability of Li-one edge ZGNR as predicted by corresponding band structures and DOS investigations.

4. Conclusions

We have systematically examined the stability aspects of Li-terminated ZGNR and revealed their potential applications in spintronic devices. It is noticed that both the structures under investigation are energetically stable and exhibit AFM ground state. Li-one edge structures are found to be more stable than that of Li-both edges. Further, Li-one edge ZGNR is metallic (semiconducting) for spin up (spin down) electrons and therefore exhibit perfect half-metallic character which is not affected by their widths. The observed half metallicity is further supported by I - V characteristics and corresponding TS calculations. The importance of present work lies in the fact that observed half-metallicity persists without application of any electric field which makes present configurations preferable for spin filtering applications.

Acknowledgements

Authors are thankful to ABV- Indian Institute of Information Technology & Management, Gwalior for utilizing its computational facilities.

References

- [1] K.S. Novoselov, A.K. Geim, S.V. Morozov, D. Jiang, Y. Zhang, S.V. Dubonos, I.V. Grigorieva, A.A. Firsov, Electric field effect in atomically thin carbon films, *Science* 306 (2004) 666–669.
- [2] A.K. Geim, K.S. Novoselov, The rise of graphene, *Nat. Mater.* 6 (2007) 183–191.
- [3] B. Standley, W. Bao, H. Zhang, J. Bruck, C.N. Lau, M. Bockrath, Graphene-based atomic-scale switches, *Nano Lett.* 8 (2008) 3345–3349.
- [4] A.H.C. Neto, F. Guinea, N.M.R. Peres, K.S. Novoselov, A.K. Geim, The electronic properties of graphene, *Rev. Mod. Phys.* 81 (2009) 109–162.
- [5] D.A. Abanin, L.S. Levitov, Quantized transport in graphene p-n junctions in magnetic field, *Science* 317 (2007) 641–643.
- [6] Y. Zhang, Y.-W. Tan, H.L. Stormer, P. Kim, Experimental observation of the quantum Hall effect and Berry's phase in graphene, *Nature* 438 (2005) 201–204.
- [7] X. Liang, S. Wi, Transport characteristics of multichannel transistors made from densely aligned sub-10 nm half-pitch graphene nanoribbons, *ACS Nano* 6 (2012) 9700–9710.
- [8] F. Schedin, A.K. Geim, S.V. Morozov, E.W. Hill, P. Blake, M.I. Katsnelson, K.S. Novoselov, Detection of individual gas molecule adsorbed on graphene, *Nat. Mater.* 6 (2007) 652–655.
- [9] X. Liang, Z. Fu, S.Y. Chou, Graphene transistors fabricated via transfer-printing in device active-areas on large wafer, *Nano Lett.* 7 (2007) 3840–3844.
- [10] W. Han, R.K. Kawakami, M. Gmitra, J. Fabian, Graphene spintronics, *Nat. Nanotechnol.* 9 (2014) 794–807.
- [11] R. Farghadan, A. Saffarzadeh, Generation of fully spin-polarized currents in three-terminal graphene-based transistors, *RSC Adv.* 5 (2015) 87411–87415.
- [12] X.Q. Deng, Z.H. Zhang, G.P. Tang, Z.Q. Fan, C.H. Yang, Spin filter effects in zigzag-edge graphene nanoribbons with symmetric and asymmetric edge hydrogenations, *Carbon* 66 (2014) 646–653.
- [13] Y.W. Son, M.L. Cohen, S.G. Louie, Half-metallic graphene nanoribbons, *Nature* 444 (2006) 347–349.
- [14] J. Kang, F. Wu, J. Li, Doping induced spin filtering effect in zigzag graphene nanoribbons with asymmetric edge hydrogenation, *Appl. Phys. Lett.* 98 (2011)

- (083109-1-083109-3).
- [15] S.L. Yan, M.Q. Long, X.J. Zhang, H. Xu, The effects of spin-filter and negative differential resistance on Fe-substituted zigzag graphene nanoribbons, *Phys. Lett. A* 378 (2014) 960–965.
 - [16] F. Zou, L. Zhu, K. Yao, Perfect spin filtering effect and negative differential behaviour in phosphorus-doped zigzag graphene nanoribbons, *Sci. Rep.* 5 (2015) (15966-1-15966-10).
 - [17] G.A. Nemnes, S. Antohe, Spin filtering in graphene nanoribbons with Mn-doped boron nitride inclusions, *Mater. Sci. Eng. B* 178 (2013) 1347–1351.
 - [18] N.K. Jaiswal, P. Srivastava, Tailoring the electronic structure of zigzag graphene nanoribbons via Cu impurities, *J. Comput. Theor. Nanosci.* 10 (2013) 1441–1445.
 - [19] B. Mandal, S. Sarkar, A. Pramanik, P. Sarkar, Doped defective graphene nanoribbons: a new class of materials with novel spin filtering properties, *RSC Adv.* 4 (2014) 49946–49952.
 - [20] M. Brandbyge, J.L. Mozos, P. Ordejon, J. Taylor, K. Stokbro, Density-functional method for nonequilibrium electron transport, *Phys. Rev. B* 65 (2002) 165401-1–165401-17.
 - [21] (www.quantumwise.com).
 - [22] H.J. Monkhorst, J.D. Pack, Special points for Brillouin-zone integrations, *Phys. Rev. B* 13 (1976) 5188–5192.
 - [23] J.P. Perdew, K. Burke, M. Ernzerhof, Generalized gradient approximation made simple, *Phys. Rev. Lett.* 77 (1996) (3865-1-3865-4).
 - [24] N.K. Jaiswal, P. Srivastava, Enhanced metallicity and spin polarization in zigzag graphene nanoribbons with Fe impurities, *Physica E* 54 (2013) 103–108.
 - [25] C. Uthaisar, D.J. Hicks, V. Barone, Li adsorption on edge-oxidized graphene nanoribbons predicted by DFT calculations, *Surf. Sci.* 619 (2014) 105–113.
 - [26] L. Pisani, J.A. Chan, B. Montanari, N.M. Harrison, Electronic structure and magnetic properties of graphitic ribbons, *Phys. Rev. B* 75 (2007) 064418-1–064418-9.
 - [27] Er-jun Kan, Z. Li, J. Yang, J.G. Hou, Half-metallicity in edge modified zigzag graphene nanoribbons, *J. Am. Chem. Soc.* 130 (2008) 4224–4225.
 - [28] M. Wu, X. Wu, Y. Gao, X.C. Zeng, Materials design of half-metallic graphene and graphene nanoribbons, *Appl. Phys. Lett.* 94 (2009) 223111-1–223111-3.
 - [29] P. Srivastava, N.K. Jaiswal, G. Tripathi, Chlorine sensing properties of zigzag boron nitride nanoribbons, *Solid State Commun.* 185 (2014) 41–46.